International Journal of Power Electronics and Drive Systems (IJPEDS)
Vol. 12, No. 1, Mar 2021, pp. 325~333
ISSN: 2088-8694, DOI: 10.11591/ijpeds.v12.i1.pp325-333

Dynamic simulation of three-phase nine-level multilevel inverter with switching angles optimized using nature-inspired algorithm

W. T. Chew[1], W. V. Yong[2], J. S. L. Ong[3], J. H. Leong[4], T. Sutikno[5]
[1,2,3,4]School of Electrical Systems Engineering, University Malaysia Perlis, Perlis, Malaysia
[5]Department of Electrical Engineering, Universitas Ahmad Dahlan, Yogyakarta, Indonesia

Article Info

Article history:

Received Jun 20, 2020
Revised Jan 19, 2021
Accepted Feb 5, 2021

Keywords:

Dynamic simulation
GA
GOA
Multilevel inverter
NR
SHMPWM

ABSTRACT

This paper recommends the use of grasshopper optimization algorithm (GOA), a nature-inspired optimization algorithm, for optimizing switching-angle applied to cascaded H-bridge multilevel inverter (CHBMLI). Switching angles are selected based on the minimum value of the objective function formulated using the concept of selective harmonic minimization pulse width modulation (SHMPWM) technique. MATLAB/Simulink-PSIM dynamic co-simulation conducted on a 3-phase 9-level CHBMLI shows that the CHBMLI controlled using GOA derived switching-angle is able to respond to varying modulation index demand and synthesize an AC staircase output voltage waveform with the desired fundamental harmonic and minimized selected low-order harmonics. Compared to Newton Raphson (NR) technique, GOA is able to find optimum switching-angle solutions over a wider modulation index range. Compared to Genetic Algorithm (GA), GOA is able to find global minima with higher probability. The simulation results validate the performance of GOA for switching-angle calculation based on the concept of SHMPWM.

Corresponding Author:

J. H. Leong
School of Electrical Systems Engineering
University Malaysia Perlis
02600 Arau, Perlis, Malaysia
Email: nick.unimap@gmail.com

1. INTRODUCTION

Nowadays, multilevel inverter (MLI) has been applied in medium-voltage and high-power applications such as active filters, electrical motor drives and photovoltaic grid-connected system [1]-[7]. Multilevel inverter has several advantages such as lower switching losses, lower voltage stress on power switches, and lower electromagnetic interference (EMI) compared to two-level high-frequency pulse-width modulation (PWM) inverter [8], [9]. There are three main MLI topologies which are diode-clamped, flying capacitor and cascaded H-bridge [6]. Among them, cascaded H-bridge multilevel inverter (CHBMLI), which has the benefits of flexibility and modularity, has gained increasing attention in wide range of applications [6], [8]. CHBMLI is controlled by applying a set of optimum switching angles to synthesize a near sinusoidal staircase output voltage waveform. However, the optimum switching angles that can provide an output voltage waveform with low total harmonic distortion (THD) are not easy to be determined [8], [9].

Several methods to control the MLI have been reported in the past. Sinusoidal PWM and space vector PWM are the common high-frequency PWM methods to control the MLI [6], [10]. However, high switching loss is the main drawback in both methods. Another method is the fundamental-frequency PWM

method which has lower switching losses [6]. Optimal minimization of total harmonic distortion (OMTHD) is one of the fundamental-frequency PWM method that can minimize the THD [11]. However, it cannot guarantee that the low-order harmonics are minimized. Selective harmonic minimization pulse-width modulation (SHMPWM) is the common fundamental-frequency PWM method that can be employed to obtain the optimum switching angles without having the problem of high switching losses [12]. SHMPWM can minimize the low-order harmonics and maintain the fundamental component at the same time. In this method, a set of non-linear transcendental equations of the selected harmonics that consist of trigonometric terms is to be solved. Newton Raphson (NR) technique is a common iterative mathematical method used to solve the equations [13]. However, NR is highly dependent on good initial switching-angle guesses and it often provides solution for a certain range of modulation index only. Another technique to solve the non-linear equations is by converting the non-linear equations to polynomial equations and then solving them using resultant theory (RT) [14]-[16]. While this technique can provide a wide range of solutions, it is computationally complex and time-consuming for high-dimension switching-angle calculation. Hence, NR and RT are rather difficult to be implemented. Another method to optimize the MLI switching angles is by employing soft-computing approach [17]. The advantage of soft-computing approach is that the algorithm usually does not require a good guess of initial switching angles. Genetic algorithm (GA), which is a well-known soft-computing method, has been applied successfully in a wide range of applications, e.g. network routing and image processing [18]. It has also been employed to optimize the switching angles of MLI [19]. However, GA is easily trapped in the local optima due to the absence of exploration and exploitation abilities. Thus, GA has lower probability to find the global minima [20].

Recently, a nature-inspired soft-computing algorithm known as grasshopper optimization algorithm (GOA) has been proposed to solve optimization problem [21]. In last few years, GOA has been applied in several applications such as electrical characterization of proton exchange membrane fuel cells stack, power quality enhancement in an isolated microgrid, color image multilevel thresholding, meta-matching approach for ontology alignment, voltage control of switched reluctance generator and optimal reconfiguration of PV array [20], [22]-[26]. The application of GOA in THD minimization of power electronic converters has rarely been reported. Therefore, GOA is proposed in this paper to determine the optimum switching angles for the MLI. Unlike NR, GOA could find optimum solutions without requiring a good initial switching angle guess. The GOA based SHMPWM has been implemented and analyzed using MATLAB, whilst the switching-angle solution is compared to that obtained using NR and GA method. A Simulink/PSIM co-simulation model has also been developed to evaluate and verify the dynamic performance of a 3-phase 9-level CHBMLI with GOA optimized switching angles under dynamic modulation index demand.

2. IMPLEMENTATION OF GOA-SHMPWM FOR 3-PHASE 9-LEVEL CHBMLI

A CHBMLI is constructed by a series of H-bridge circuits. Each H-bridge circuit consists of a DC voltage source and four power semiconductor switches that are able to produce voltage levels $+V_{dc}$, *0* or $-V_{dc}$. A *(2k+1)*-level of staircase output phase voltage waveform can be produced by a combination of *k* number of H-bridge circuits. Figure 1(a) shows the construction of one of the phases and Figure 1(b) shows the output phase voltage waveform synthesized from four H-bridge circuits. In this paper, the phases of the CHBMLI are connected to form a balanced 3-phase Y-connection circuit with 120˚ of phase shift. Based on Figure 1(b), the output phase voltage waveform could be represented in Fourier series as (1) [7]:

$$V_{ph}(t) = \sum_{n=1}^{\infty} \frac{4V_{dc}}{n\pi} [cos(n\alpha_1) + cos(n\alpha_2) + cos(n\alpha_3) + cos(n\alpha_4)] \, sin(n\omega t) \quad (1)$$

where *n* is always an odd number and it also represents the *n*-th harmonics, V_{dc} represents the magnitude of DC voltage source in each H-bridge circuit, and ω is the angular frequency of the fundamental harmonic. The switching angles α_1, α_2, α_3 and α_4 are in unit radian and must satisfy the condition of $0 \le \alpha_1 \le \alpha_2 \le \alpha_3 \le \alpha_4 \le \pi/2$ [19]. From (1), the *n*-th harmonic can be expressed as (2) [7]:

$$V_n = \frac{4V_{dc}}{n\pi} [cos(n\alpha_1) + cos(n\alpha_2) + cos(n\alpha_3) + cos(n\alpha_4)] \quad (2)$$

The objective of the SHMPWM is to minimize the undesired low-order harmonics and maintain the desired fundamental component of output voltage waveform. In a balanced 3-phase 9-level CHBMLI, 5th, 7th and 11th harmonics are chosen to be minimized while the first harmonic is maintained at the desired value. The triplen odd harmonis are not required to be minimized because they are eliminated naturally in the 3-phase system. In this paper, GOA is applied in SHMPWM to optimize the switching angles.

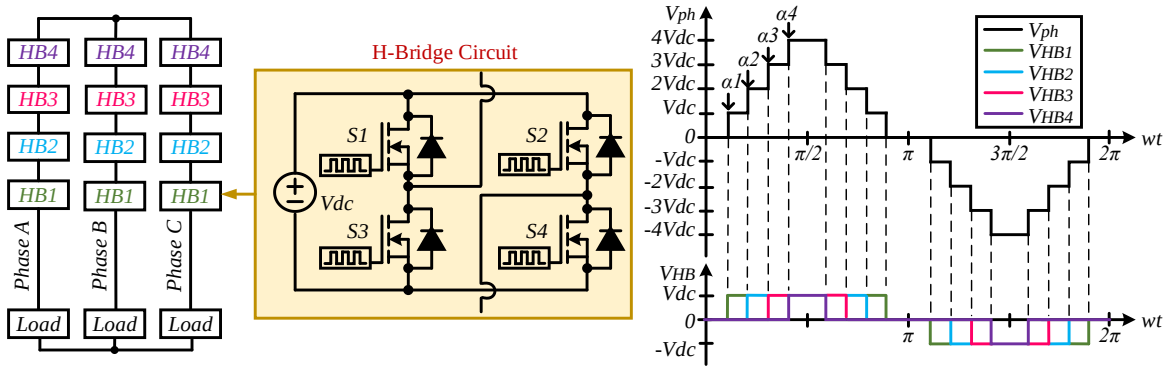

Figure 1. Block diagram showing a 3-phase 9-level CHBMLI and typical phase voltage waveform

GOA is a population-based nature-inspired algorithm which is based on the swarm behavior of grasshoppers. The algorithm mimics the movements of the grasshoppers in migration and food foraging process. The mathematical model for implementing the movement of grasshoppers is given by (3) [21]:

$$X_i^d = c\left[\sum_{\substack{j=1 \\ j\neq i}}^{N} c\,\frac{ubd-lbd}{2}\,s\left(\left|x_j^d - x_i^d\right|\right)\frac{x_j^d - x_i^d}{d_{ij}}\right] + T_d \quad (3)$$

where *ubd* is the upper bound in the *d-th* dimension, *lbd* is the lower bound in the *d-th* dimension, T_d is the best target value and d_{ij} is the distance between *i-th* grasshopper and *j-th* grasshopper. The *c* is a decreasing coefficient which is expressed as (4) [21]:

$$c = c(cmin_{max}/iter_{min})_{max} \quad (4)$$

where c_{max} is the maximum value of the coefficient, c_{min} is the minimum value of coefficient, *iter* is the current number of iteration and $iter_{max}$ is the maximum number of iterations. The function *s* is the social force used to decide the movement of grasshopper and it is presented as (5) [21]:

$$s(r) = fe^{-r/l} - e^{-r} \quad (5)$$

where *r* is the normalized distance between *i-th* and *j-th* grasshoppers, *l* is the attractive length scale and *f* is the intensity of attraction. An objective function (OF), which is used in the GOA-SHMPWM to minimize the undesired harmonics and maintain the desired fundamental component, is adapted from [19] as (6):

$$OF = \left(100 \times \frac{V_D - V_1}{V_D}\right)^4 + \frac{1}{5}\left(\frac{50V_5}{V_1}\right)^2 + \frac{1}{7}\left(\frac{50V_7}{V_1}\right)^2 + \frac{1}{11}\left(\frac{50V_{11}}{V_1}\right)^2 \quad (6)$$

where $V_D = (4kMV_{dc})/\pi$ is desired fundamental harmonic that is controlled by the modulation index, *M*, and V_1, V_5, V_7 and V_{11} are fundamental, 5th, 7th and 11th harmonics of the phase voltage waveform, respectively. The first term of (6) is used to regulate the desired fundamental harmonics, whilst the same time the second, third and forth terms are used to reduce the 5th, 7th and 11th harmonics, respectively. The objective of the first term is to limit the relative error between the V_D and V_1 by 1%. For the second, third and forth terms, the 5th, 7th and 11th harmonics are kept under 2% of the fundamental harmonic. Therefore, all desired conditions could be controlled with the proposed OF while the optimum solution for all modulation index could be determined by using the implementation of GOA. Based on (2), V_1, V_5, V_7 and V_{11} can be expressed as (7):

$$V_1 = \frac{4V_{dc}}{\pi}\left[\cos(\alpha_1)+\cos(\alpha_2)+\cos(\alpha_3)+\cos(\alpha_4)\right]$$
$$V_5 = \frac{4V_{dc}}{5\pi}\left[\cos(5\alpha_1)+\cos(5\alpha_2)+\cos(5\alpha_3)+\cos(5\alpha_4)\right]$$
$$V_7 = \frac{4V_{dc}}{7\pi}\left[\cos(7\alpha_1)+\cos(7\alpha_2)+\cos(7\alpha_3)+\cos(7\alpha_4)\right]$$
$$V_{11} = \frac{4V_{dc}}{11\pi}\left[\cos(11\alpha_1)+\cos(11\alpha_2)+\cos(11\alpha_3)+\cos(11\alpha_4)\right] \quad (7)$$

GOA-SHMPWM has been implemented using MATLAB to calculate the optimum switching angles, while the implementation of GOA-SHMPWM is illustrated in Figure 2. In the GOA-SHMPWM implementation, the parameters used for GOA are as follows: $l = 1.5$, $f = 0.5$, $c_{min} = 0.00001$, $c_{max} = 0.5$, $N = 100$ and $iter_{max} = 100$. Switching-angle calculation is performed for a 3-phase 9-level CHBMLI for modulation index range from 0.01 to 1.00 in step size of 0.01.

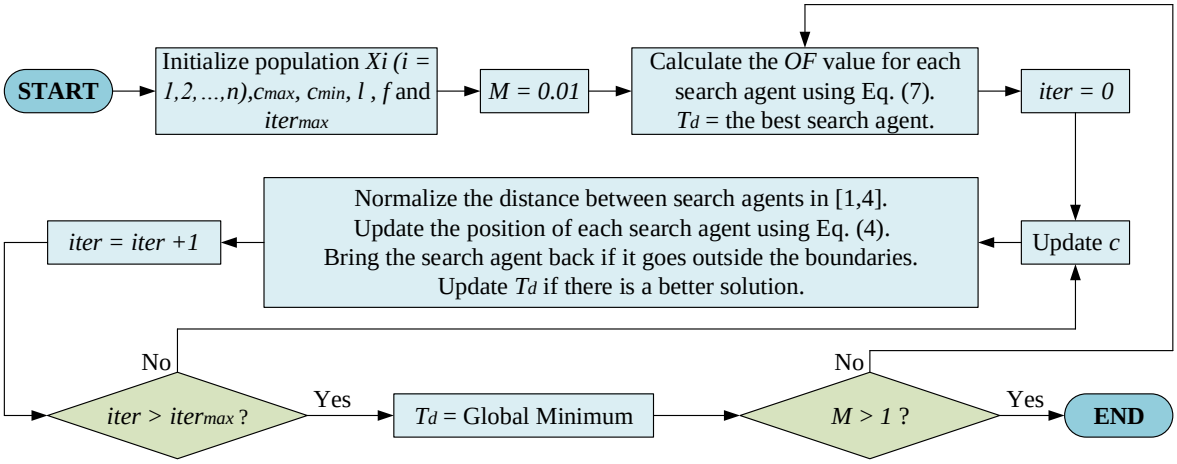

Figure 2. Flowchart of GOA-SHMPWM implementation in a wide modulation index range

In order to validate whether the CHBMLI controlled using GOA-SHMPWM optimum switching angles is capable to respond to the change of modulation index demand, a dynamic co-simulation of MATLAB/SIMULINK-PSIM is implemented on 3-phase 9-level CHBMLI. Figure 3 shows the Simulink model of switching-angle generator for 3-phase 9-level CHBMLI, whilst Figure 4 shows the block diagram of 3-phase 9-level CHBMLI simulation model and its PSIM implementation. Prior to the simulation, the switching angles that are optimized by GOA-SHMPWM are stored in look-up tables as shown in Figure 3. During simulation, the optimized switching angles are interpolated from the look-up tables based on the dynamically changing modulation index demand. The switching angles are distributed into 24 signals (g1 to g24) through gate signal generator. By using the SimCoupler interface as shown in Figure 3, the 24 signals are linked to the PSIM 3-phase 9-level CHBMLI simulation model as shown in Figure 4. Each H-bridge module employs a 12V DC voltage source and the CHBMLI is switched at 50Hz. Output voltage waveforms are generated from the simulation model based on the modulation index demand.

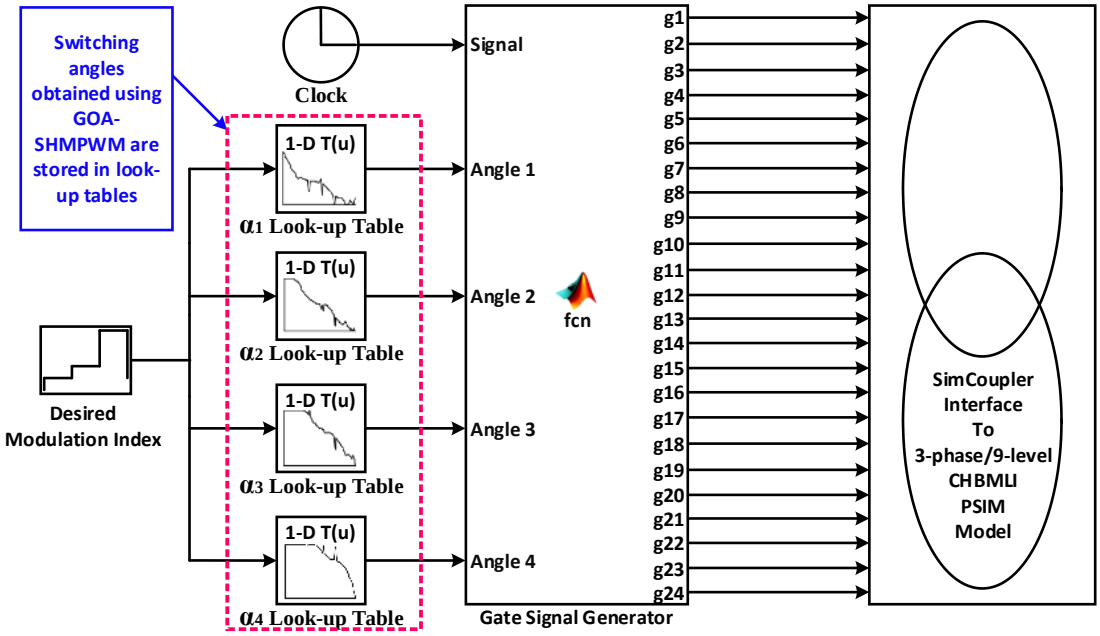

Figure 3. Simulink model of switching-angle generator for 3-phase 9-level CHBMLI

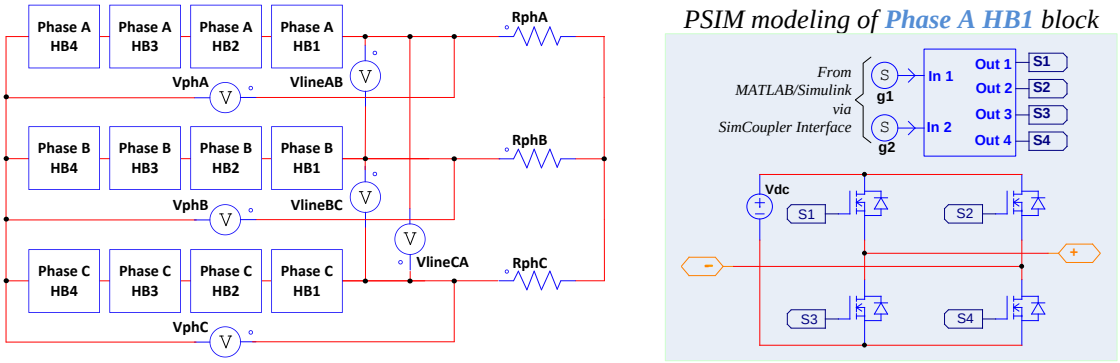

Figure 4. Block diagram of 3-phase 9-level CHBMLI simulation model and its PSIM implementation

3. RESULTS AND DISCUSSION

Switching angles obtained from GOA are benchmarked against those obtained from NR technique and GA, as shown in Figure 5. Compared to NR as shown in Figure 5(a), GOA in Figure 5(b) has a wider modulation index range of optimum switching-angle solutions. Figure 6(a) shows the minimum OF achieved by GA and GOA for the modulation index range investigated. As shown in Figure 6(a), GOA mostly achieves lower OF compared to GA in a wide range of modulation index. As shown in Figure 6(b), 38% of the modulation index range achieves a minimum OF of 10^{-2} and below by using GA, and 38% of the modulation index range achieves a minimum OF of 10^{-8} and below by using GOA. This result suggests that GOA has a higher probability than GA to reach global minima in the CHBMLI optimization search space and the undesired 5th, 7th and 11th harmonics are nearly eliminated. As a result, GOA is able to produce higher accuracy of optimum switching angles than GA. Figure 6(c) shows the phase voltage THD and line-to-line voltage THD of the CHBMLI that achieved by GOA. The line-to-line voltage THD is always lower than the phase voltage THD because of the natural elimination of triplen harmonics in line-to-line voltage waveform. Based on Figure 6(c), the lowest phase voltage THD that can be achieved by GOA is 9.65% for M = 0.82.

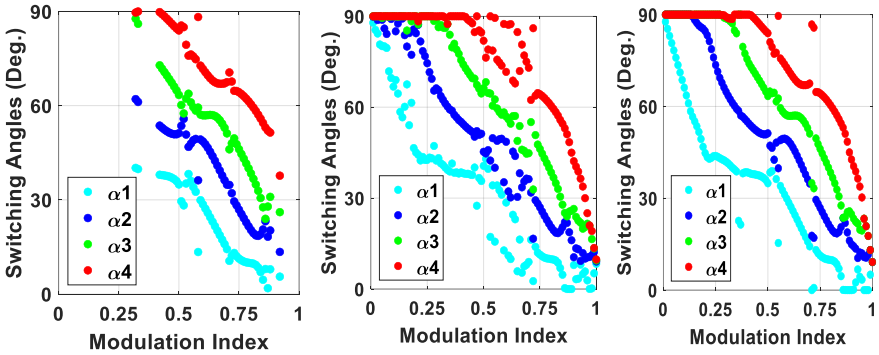

Figure 5. Switching angles derived using (a) NR, (b) GA, (c) GOA techniques

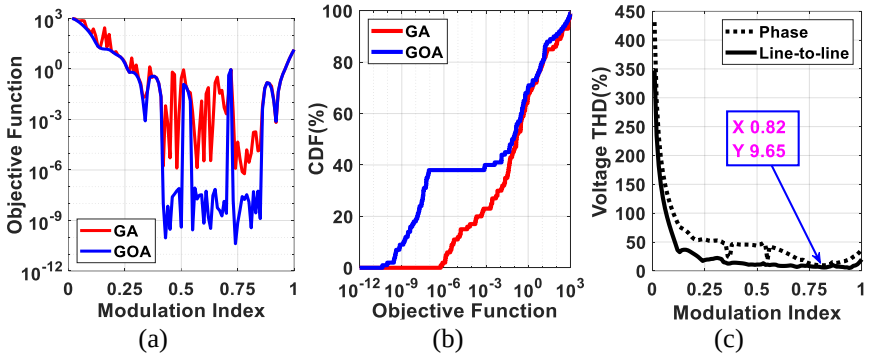

Figure 6. MATLAB analysis: (a) OF (GOA vs GA), (b) CDF (GOA vs GA), (c) Voltage THD (GOA)

Table 1 shows the selected modulation indexes demand for the dynamic co-simulation, whilst Figure 7 shows the stepped modulation index demand, phase voltage waveforms and line-to-line voltage waveforms obtained from MATLAB/Simulink-PSIM dynamic co-simulation. The modulation index is varied at every 0.1s time interval. From 0 to 0.4s, when the modulation index is increased from 0.13 to 0.82, the voltage level increases from 3-level to 9-level and the peak phase voltage increases from 12V to 48V. At 0.4s, the modulation index is decreased from 0.82 to 0.27, the voltage level decreases 9-level to 5-level and the peak phase voltage decreases from 48V to 24V. Due to the three-phase configuration, a 120˚ phase shift with respect to the adjacent leg is observed in the output phase voltage and line-to-line voltage waveforms. These results verify that the CHBMLI controlled using the GOA-SHMPWM optimized switching angles is capable to respond the change of modulation index demand.

Close-up view of phase and line-to-line voltage waveforms for each modulation index demand are shown in Table 2. Fast Fourier Transform (FFT) are applied in the phase and line-to-line voltage waveforms for each modulation index to show the harmonic contents. Table 2 shows the voltage waveforms and FFT analysis for M = 0.13, M = 0.27, M = 0.41 and M = 0.82, respectively. The magnitudes of V_1 are 7.99V, 16.54V, 25.10V and 50.10V, which are very close to V_D of 7.95V, 16.50V, 25.06V and 50.11V as listed in Table 1, respectively, for M = 0.13, M = 0.27, M = 0.41 and M = 0.82, respectively. In addition, the magnitude of fundamental harmonic of the line-to-line voltage waveform for each modulation index is approximately $\sqrt{3}\times V_1$. For M = 0.27, M = 0.41 and M = 0.82, the chosen 5th, 7th and 11th harmonics in the phase and line voltage waveforms are nearly eliminated. This is reasonable since the OF related with these modulation indexes are successfully minimized, which can be confirmed in Figure 6(a). Nevertheless, the 5th, 7th and 11th harmonics of the voltage waveforms for M = 0.13 are only reduced as much as possible due to the low modulation index of output voltage waveform that has the lowest number of voltage levels. Table 3 compares the MATLAB and dynamic simulation results of fundamental harmonic, phase voltage THD and line-to-line voltage THD for each modulation index demand. It can be observed that the results between MATLAB and dynamic simulation are very close.

In order to demonstrate that the CHBMLI controlled using GOA-SHMPWM switching angles is able to produce a steady output waveform during the load change, the load impedance is dynamically varied in the simulation. Figure 8 shows the change of phase voltage waveform and load current waveform during the dynamic load change at 0.1s for modulation index *M = 0.82*. Before 0.1s, the impedance is 1Ω and power factor is 0.81 while the peak value of the phase voltage and load current is 48V and 51.91A, respectively. After 0.1s, the impedance is 0.72Ω and power factor is 0.57, whilst the peak phase voltage and load current is 48V and 74.86A, respectively. This figure shows that the peak value of the load current increases during the load change and the phase voltage waveform still remain the same after the load change.

Table 1. Optimum switching angles and number of phase voltage levels of selected modulation index used for 3-phase 9-level CHBMLI MATLAB/Simulink-PSIM dynamic co-simulation

M	V_D (V)	α_1 (deg.)	α_2 (deg.)	α_3 (deg.)	α_4 (deg.)	Num. of voltage levels
0.13	7.95	58.46	90.00	90.00	90.00	3
0.27	16.50	41.89	67.77	90.00	90.00	5
0.41	25.06	25.05	51.62	64.31	90.00	7
0.82	50.11	8.63	19.22	34.69	58.34	9

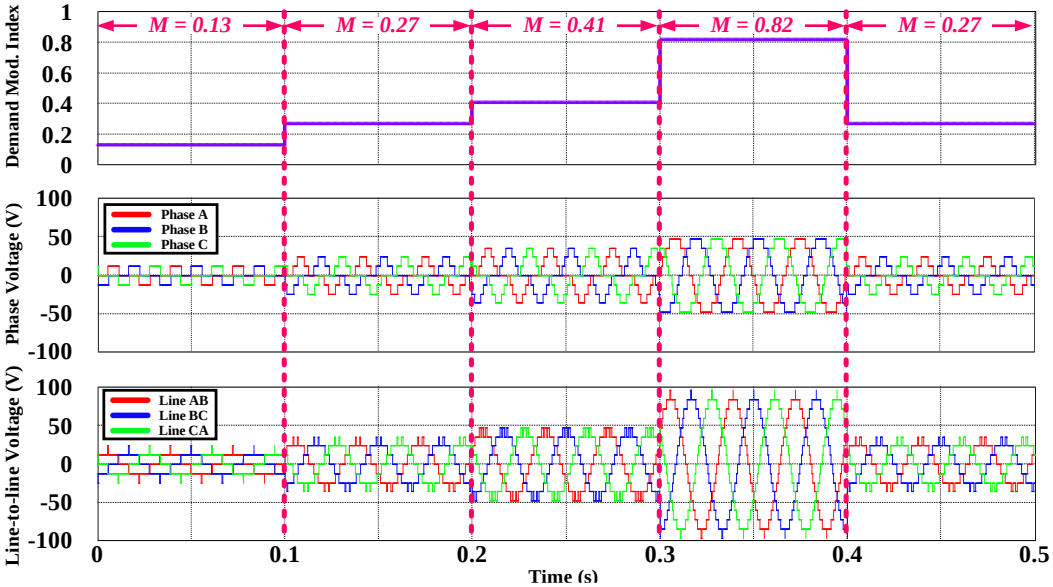

Figure 7. Stepped modulation index demand at every 0.1s interval, phase voltage waveforms and line-to-line voltage waveforms obtained from MATLAB/Simulink-PSIM dynamic co-simulation

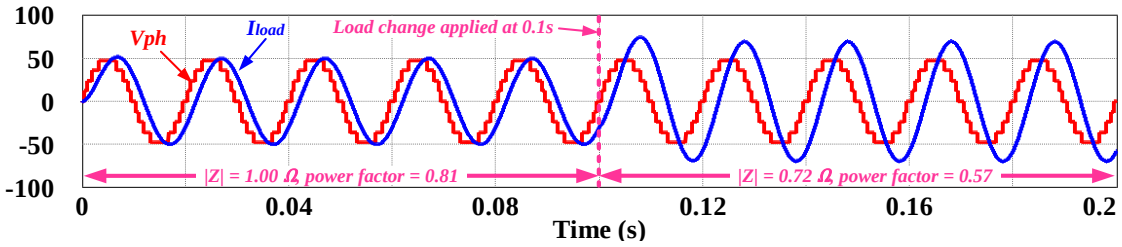

Figure 8. Dynamic load change is applied at 0.1s (*|Z| is load impedance; M = 0.82*)

Table 2. Closed-up view of simulated output voltage waveforms and FFT analysis

M	Dynamic Co-Simulation Results Phase and Line Voltage Waveforms *[voltage (V) vs time (s)]*	Phase Voltage FFT Analysis *[harmonic amplitude (V) vs freq. (Hz)]*	Line Voltage FFT Analysis *[harmonic amplitude (V) vs freq. (Hz)]*
0.13	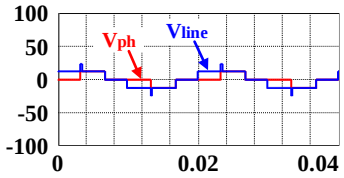	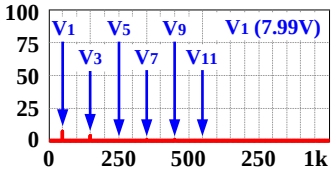	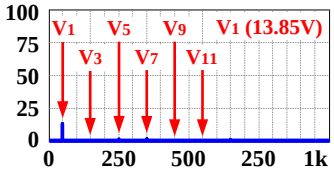
0.27	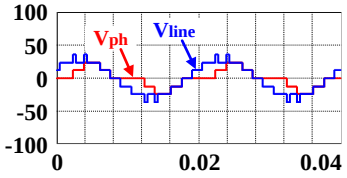	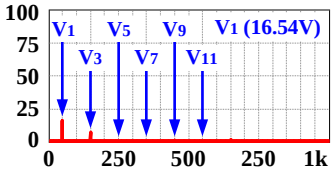	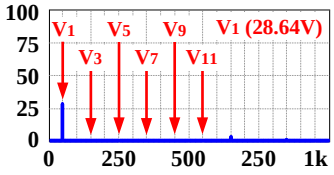
0.41	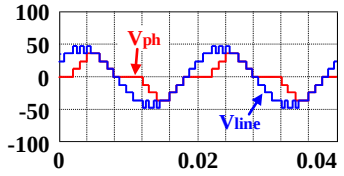	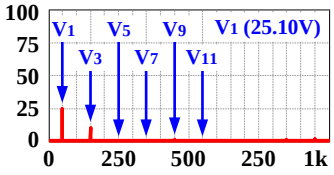	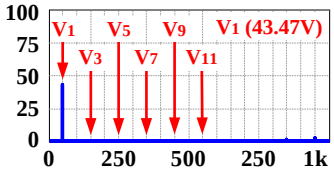
0.82	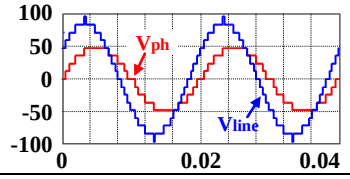	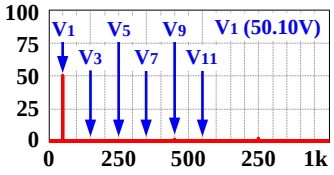	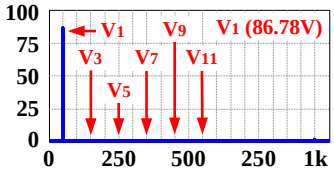

Table 3. Fundamental harmonic, phase voltage THD and line-to-line voltage THD comparison between MATLAB calculation result and PSIM simulation result

Comparison		MATLAB Analysis Result	Dyn. Co-Sim. Result	Difference
M = 0.13	V_1 (V)	7.99	7.99	0.00
	V_{ph} THD (%)	76.13	76.11	0.02
	V_{line} THD (%)	32.41	32.38	0.03
M = 0.27	V_1 (V)	16.54	16.54	0.00
	V_{ph} THD (%)	52.24	52.25	0.01
	V_{line} THD (%)	19.74	19.74	0.00
M = 0.41	V_1 (V)	25.11	25.10	0.01
	V_{ph} THD (%)	45.97	45.97	0.00
	V_{line} THD (%)	13.74	13.75	0.01
M = 0.82	V_1 (V)	50.11	50.10	0.01
	V_{ph} THD (%)	9.65	9.66	0.01
	V_{line} THD (%)	5.80	5.80	0.00

4. CONCLUSION

In this paper, the performance of GOA for optimizing switching angles applied to dynamic simulation of 3-phase 9-level CHBMLI have been presented. The switching angle results show that GOA has a wider range of optimized switching-angle solutions than NR technique. The OF and CDF results show that GOA is able to determine the optimum switching angles with higher accuracy compared to GA. Thus, GOA has superior performance over NR and GA in the MLI control. In addition, the MATLAB/Simulink-PSIM dynamic co-simulation result verifies that the CHBMLI can respond to the change of modulation index demand and generate output voltage waveforms with minimized selected harmonics and desired fundamental component. Furthermore, the simulation result of dynamic load change validates that CHBMLI with GOA-SHMPWM switching angles is able to produce a steady output phase voltage under dynamic load change.

ACKNOWLEDGEMENTS

This work was supported by the Ministry of Education Malaysia through the Fundamental Research Grant Scheme (FRGS/1/2017/TK07/UNIMAP/02/2).

REFERENCES

[1] H. Abu-Rub, J. Holts, J. Rodriguez, and G. Baoming, "Medium voltage multilevel converters, state of the art, challenges and requirements in industrial applications," *IEEE Transactions on Industrial Electronics*, vol. 57, no. 8, pp. 2581–2596, Aug. 2010.

[2] F. H. Khan, L. M. Tolbert, and W. E. Webb, "Hybrid Electric Vehicle Power Management Solutions Based on Isolated and Nonisolated Configurations of Multilevel Modular Capacitor-Clamped Converter," *IEEE Transactions on Industrial Electronics*, vol. 56, no. 8, pp. 3079–3095, Aug. 2009.

[3] I. J. Hasan, N. Abdul, J. Salih, and N. I. Abdulkhaleq, "Three-phase photovoltaic grid inverter system design based on PIC24FJ256GB110 for distributed generation," *International Journal of Power Electronics and Drive Systems (IJPEDS)*, vol. 10, no. 3, pp. 1215–1222, 2019.

[4] C. Laoufi, Z. Sadoune, A. Abbou, and M. Akherraz, "New model of electric traction drive based sliding mode controller in field-oriented control of induction motor fed by multilevel inverter," *International Journal of Power Electronics and Drive Systems (IJPEDS)*, vol. 11, no. 1, pp. 242–250, 2020.

[5] G. V. Nagaraju and G. S. Rao, "Three phase PUC5 inverter fed induction motor for renewable energy applications," *International Journal of Power Electronics and Drive Systems (IJPEDS)*, vol. 11, no. 1, pp. 1–9, 2020.

[6] J. Rodriguez, J. S. Lai, and F. Z. Peng, "Multilevel inverters: a survey of topologies, controls, and applications," *IEEE Transactions on Industrial Electronics*, vol. 49, no. 4, pp. 724–738, Aug. 2002.

[7] L. M. Tolbert, F. Z. Peng, and T. G. Habetler, "Multilevel converters for large electric drives," *IEEE Transactions on Industry Applications*, vol. 35, no. 1, pp. 36–44, 1999.

[8] M. Malinowski, K. Gopakumar, J. Rodriguez, and M. A. Pérez, "A Survey on Cascaded Multilevel Inverters," *IEEE Transactions on Industrial Electronics*, vol. 57, no. 7, pp. 2197–2206, Jul. 2010.

[9] L. G. Franquelo, J. Rodriguez, J. I. Leon, S. Kouro, R. Portillo, and M. A. M. Prats, "The age of multilevel converters arrives," *IEEE Industrial Electronics Magazine*, vol. 2, no. 2, pp. 28–39, Jun. 2008.

[10] A. K. Gupta and A. M. Khambadkone, "A Space Vector PWM Scheme for Multilevel Inverters Based on Two-Level Space Vector PWM," *IEEE Transactions on Industrial Electronics*, vol. 53, no. 5, pp. 1631–1639, Oct. 2006.

[11] N. Yousefpoor, S. Fathi, N. Farokhnia, and H. Abyaneh, "THD Minimization Applied Directly on the Line-to-Line Voltage of Multilevel Inverters," *IEEE Transactions on Industrial Electronics*, vol. 59, no. 1, pp. 373–380, 2012.

[12] G. Konstantinou, M. Ciobotaru, and V. Agelidis, "Selective harmonic elimination pulse-width modulation of modular multilevel converters," *IET Power Electronics*, vol. 6, no. 1, pp. 96–107, Jan. 2013.

[13] R. M. Hossam, G. M. Hashem, and M. I. Marei, "Optimized harmonic elimination for cascaded multilevel inverter," *48th International Universities' Power Engineering Conference (UPEC), Dublin*, pp. 1–6, 2013.

[14] J. N. Chiasson, L. M. Tolbert, K. J. McKenzie, and Z. Du, "Control of a multilevel converter using resultant theory," *IEEE Transactions on Control Systems Technology*, vol. 11, no. 3, pp. 345-354, May 2003, doi: 10.1109/TCST.2003.810382.

[15] J. N. Chiasson, L. M. Tolbert, K. J. McKenzie, and Zhong Du, "A complete solution to the harmonic elimination problem," *IEEE Transactions on Power Electronics*, vol. 19, no. 2, pp. 491–499, Mar. 2004.

[16] J. N. Chiasson, L. M. Tolbert, K. J. McKenzie, and Zhong Du, "Elimination of harmonics in a multilevel converter using the theory of symmetric polynomials and resultants," *IEEE Transactions on Control Systems Technology*, vol. 13, no. 2, pp. 216–223, Mar. 2005.

[17] B. Choudhury and R. M. Jha, "Soft Computing techniques," Soft Computing in Electromagnetics: Methods and Applications, Cambridge: Cambridge University Press, pp. 9–44, 2016.

[18] A. Lambora, K. Gupta, and K. Chopra, "Genetic Algorithm- A Literature Review," *International Conference on Machine Learning, Big Data, Cloud and Parallel Computing (COMITCon)*, Faridabad, India, 2019, pp. 380–384.

[19] N. Farokhnia, S. Fathi, R. Salehi, G. Gharehpetian, and M. Ehsani, "Improved selective harmonic elimination pulse-width modulation strategy in multilevel inverters," *IET Power Electronics*, vol. 5, no. 9, pp. 1904–1911, 2012.

[20] Z. Lv and R. Peng, "A novel meta-matching approach for ontology alignment using grasshopper optimization," *Knowledge-Based Systems*, vol. 201–202, Aug. 2020.

[21] S. Saremi, S. Mirjalili, and A. Lewis, "Grasshopper Optimisation Algorithm: Theory and application," *Advances in Engineering Software*, vol. 105, pp. 30–47, Mar. 2017.

[22] A. El-Fergany, "Electrical characterisation of proton exchange membrane fuel cells stack using grasshopper optimiser," *IET Renewable Power Generation*, vol. 12, no. 1, pp. 9–17, Jan. 2018.

[23] H. Elmetwaly, A. A. Eldesouky, and A. A. Sallam, "An Adaptive D-FACTS for Power Quality Enhancement in an Isolated Microgrid," *IEEE Access*, vol. 8, pp. 57923–57942, 2020.

[24] A. K. Bhandari and K. Rahul, "A novel local contrast fusion-based fuzzy model for color image multilevel thresholding using grasshopper optimization," *Applied Soft Computing Journal*, vol. 81, Aug. 2019.

[25] M. Bahy, *et al*., "Voltage control of switched reluctance generator using grasshopper optimization algorithm," *International Journal of Power Electronics and Drive System (IJPEDS)*, vol. 11, no. 1, pp. 75–85, 2020.

[26] A. Fathy, "Recent meta-heuristic grasshopper optimization algorithm for optimal reconfiguration of partially shaded PV array," *Solar Energy*, vol. 171, pp. 638–651, Sep. 2018.